mua-3, a gene required for mechanical tissue integrity in *Caenorhabditis elegans*, encodes a novel transmembrane protein of epithelial attachment complexes

Mark Bercher,[1] Jim Wahl,[1] Bruce E. Vogel,[2] Charles Lu,[2] Edward M. Hedgecock,[2] David H. Hall,[3] and John D. Plenefisch[1]

[1]Department of Biology, University of Toledo, Toledo, OH 43606
[2]Department of Biology, Johns Hopkins University, Baltimore, MD 21218
[3]Center for *Caenorhabditis elegans* Anatomy, Department of Neuroscience, Albert Einstein College of Medicine, New York, NY 10461

Normal locomotion of the nematode *Caenorhabditis elegans* requires transmission of contractile force through a series of mechanical linkages from the myofibrillar lattice of the body wall muscles, across an intervening extracellular matrix and epithelium (the hypodermis) to the cuticle. Mutations in *mua-3* cause a separation of the hypodermis from the cuticle, suggesting this gene is required for maintaining hypodermal–cuticle attachment as the animal grows in size postembryonically. *mua-3* encodes a predicted 3,767 amino acid protein with a large extracellular domain, a single transmembrane helix, and a smaller cytoplasmic domain. The extracellular domain contains four distinct protein modules: 5 low density lipoprotein type A, 52 epidermal growth factor, 1 von Willebrand factor A, and 2 sea urchin-enterokinase-agrin modules. MUA-3 localizes to the hypodermal hemidesmosomes and to other sites of mechanically robust transepithelial attachments, including the rectum, vulva, mechanosensory neurons, and excretory duct/pore. In addition, it is shown that MUA-3 colocalizes with cytoplasmic intermediate filaments (IFs) at these sites. Thus, MUA-3 appears to be a protein that links the IF cytoskeleton of nematode epithelia to the cuticle at sites of mechanical stress.

Introduction

Mechanical coupling between adjacent tissues in living organisms depends on the localized assembly of junctional complexes that transduce force across cell boundaries. These molecular complexes link the cytoskeleton of individual cells with those of adjacent cells or to the surrounding extracellular matrix, forming structural pathways through which mechanical force is transmitted between cells and tissues. Their integrity is critical for tissue architecture, morphogenesis, mechanical properties, and in facilitating cell–cell communication (for review see Hynes, 1999). Mutations that disrupt junctional complexes between cells and the matrix have been shown to result in developmental abnormalities in *Drosophila, Caenorhabditis elegans*, and vertebrates (for examples see Williams and Waterston, 1994; Prout et al., 1997; Henry and Campbell, 1998). In humans, congenital or acquired disruption of cell junctional complexes is associated with a wide variety of diseases, including blistering skin diseases, muscular dystrophies, neuronal dysfunction, and metastatic cancer (Campbell, 1995; Fuchs and Cleveland, 1998; Kamiguchi et al., 1998; Perl et al., 1998; Diaz and Giudice, 2000).

In vertebrates, desmosomes mechanically link the intermediate filaments (IFs)* of adjacent cells into an integrated stress-resistant path, whereas hemidesmosomes link IFs to the basal lamina (Kowalczyk et al., 1999; Nievers et al., 1999). Cell–cell and cell–matrix adherens junctions link actin filaments to adjacent cells and extracellular matrix, respectively (Hynes, 1999). The macromolecules that form

Address correspondence to John Plenefisch, Department of Biology, University of Toledo, Toledo, OH 43606-3390. Tel.: (419) 530-1551. Fax: (419) 530-7737. E-mail: jplenef@uoft02.utoledo.edu

M. Bercher's present address is Pfizer Global Research and Development, Ann Arbor, MI 48105. J. Wahl's present address is University of Nebraska Medical Center, Omaha, NE 68198. B. Vogel's present address is University of Maryland Biotechnology Institute, Baltimore, MD 21201. C. Lu's present address is Department of Molecular Biology and Biochemistry, Rutgers University, Piscataway, NJ 08855.

Key words: *Caenorhabditis elegans*; cell-adhesion; extracellular matrix receptors; epidermis; intermediate filaments

*Abbreviations used in this paper: DIC, differential interference contrast; EC, calcium-binding EGF; IF, intermediate filament; LA, low density lipoprotein A module; RT, reverse transcription; SE, sea urchin-agrin-enterokinase module; SL1, spliced leader 1; TEM, transmission electron microscopy; VA, von Willebrand factor A module.

these adhesive structures are conserved among the vertebrates. For example, proteins of the integrin type appear to be the primary transmembrane mediators of cell–matrix attachment, with α6β4 associated with hemidesmosomes and β1-containing integrins associated with matrix adherens junctions, whereas cadherin family molecules are the primary transmembrane mediators of adhesion in desmosomes and cell–cell adherens junctions (for review see Hynes, 1999). Characteristic cytoplasmic adapter proteins couple these junctional receptors to the cytoskeleton.

Cytoskeletal matrix junctions with morphological similarities to those seen in vertebrates have been identified in invertebrates, including *Drosophila* and *Caenorhabditis elegans*. By ultrastructural criteria, these appear generally similar to the vertebrate adhesions, although novel junctional types have also been described (Francis and Waterston, 1991; Tepass and Hartenstein, 1993). However, even where morphological and apparent functional similarity is observed, the specific molecular composition may vary between phyla, reflecting variant selective pressures and evolutionary history.

One of the best studied examples of invertebrate junctional complexes are those associated with the transmission of skeletal muscle force across the epidermis to the cuticle of *C. elegans*. The body wall muscles are arranged in four longitudinal bands, two dorsal and two ventral, running the length of the animal adhering to and separated from the epidermis by a basal lamina (for review see Waterston, 1988; Moerman and Fire, 1997). The myofilament lattice of the muscle cells is mechanically coupled to the sarcolemma and basal lamina at the M line and dense bodies by integrins (Williams and Waterston, 1994; Gettner et al., 1995). The epidermis of the nematode, the hypodermis, rests on the basal lamina separating it from muscle, and secretes the cuticle from its apical surface (White, 1988; Kramer, 1997). In the regions of muscle contact the hypodermis becomes tightly compressed and contains organized IF arrays (Hresko et al., 1994, 1999). Junctional complexes associated with these IFs, structurally similar to hemidesmosomes, are observed at the sites of muscle–hypodermal apposition interfacing with both the basal lamina and the cuticle, and are required for force transmission (Moerman and Fire, 1997; Waterston, 1988; Hresko et al., 1999).

In vertebrates, many of the molecules that contribute to the mechanical pathway linking cytoplasmic IFs to the basal lamina via hemidesmosomes were identified by their involvement in tissue fragility diseases (Fuchs and Cleveland, 1998). To identify the molecules comprising *C. elegans* adhesion complexes between muscle and cuticle, or required for their developmental regulation, mutations that showed abnormal tissue fragility in response to mechanical stress were isolated (Plenefisch et al., 2000). Here we show that one of these genes, *mua-3*, is required at the apical hypodermal surface; mutations in *mua-3* result in the separation of hypodermis from cuticle. The MUA-3 protein is shown to be a novel transmembrane protein that localizes to hypodermal hemidesmosomes at the sites of skeletal muscle contact and to other epithelial sites where stress-resistant cuticular adhesion is required. Finally, we show that MUA-3 colocalizes with cytoplasmic IFs in the hypodermis, suggesting that it may physically link IFs to the cuticle.

Results

mua-3 is required for postembryonic adhesion of the hypodermis to the cuticle

Mutations in *mua-3* result in the detachment of the skeletal muscles from the body wall (Figs. 1 and 2; Plenefisch et al., 2000). Alleles range in severity from virtually complete muscle detachment in early larvae to partial detachment in late larvae and adults. Detachment typically initiates at a single site and progresses to include most or all of the affected muscle. Initial detachment usually occurs at the anterior tip of the worm or in the region of rectum, sites that may experience greater stress on attachment structures during normal use than elsewhere along the body wall. Eight of the alleles show detachment as early as the L1 stage. The *rh169* allele shows a later onset (L2 or L3), but a similar pattern of phenotypic progression (Plenefisch et al., 2000). *rh195* is the only viable *mua-3* allele. About 30% of *rh195* adult homozygotes show limited muscle detachment in the region of the head or the rectum (Fig. 1, C–G). In *rh195* animals, apparent separation between hypodermis and cuticle is seen at sites of muscle detachment. Interestingly, 7% of *rh169* and 1% of *rh195* L1 animals show abnormal bulges in the head, a phenotype previously reported for animals with abnormal hypodermal cell positioning and enclosure (Costa et al., 1998).

Transmission electron microscopy (TEM) observations of detachment zones in *rh195* adult animals demonstrated conclusively that *mua-3* is required for apical hypodermal attachment to the cuticle (Fig. 2). In mutant animals, the distance between apical hypodermal surface and the basal cuticle layer is consistently greater than in wild-type animals, including regions where muscles appear to remain attached to the body wall (compare Figs. 2 A and 3 B). No difference in the distance between basal hypodermal surface and the musculature is observed. In addition, muscle organization is normal. In regions where muscles pull away from the cuticle, large gaps between the apical hypodermal surface and the cuticle are observed, whereas the basal hypodermal surface still remains closely apposed to the musculature (Fig. 2 C). In these detachment zones the hypodermal compression associated with the intact hemidesmosome–IF complexes is also typically lost, the hypodermal cytoplasm expanding to fill much of the available space between detached muscle and cuticle. Muscle cells in the regions of detachment retract away from the body wall resulting in disorganization of dense body positioning. These observations suggest that MUA-3 acts at the apical hypodermal surface to maintain the attachment of the hypodermis to the basal cuticle and that the primary defect in *mua-3* mutants is the failure of these attachments.

mua-3 encodes a transmembrane protein of 3,767 amino acids with multiple EGF domains

A single cosmid containing *C. elegans* genomic DNA, F55E6, that was able to complement *mua-3* when reintroduced into *mua-3*–mutant animals was identified (see Materials and methods and Fig. 8). The F55E6 sequence contains open reading frames spread over 20 kb that could code for a single large protein. Overlapping cosmids that contain only a portion of this gene fail to rescue, whereas plasmid pOT22, which contains only the single gene and its pro-

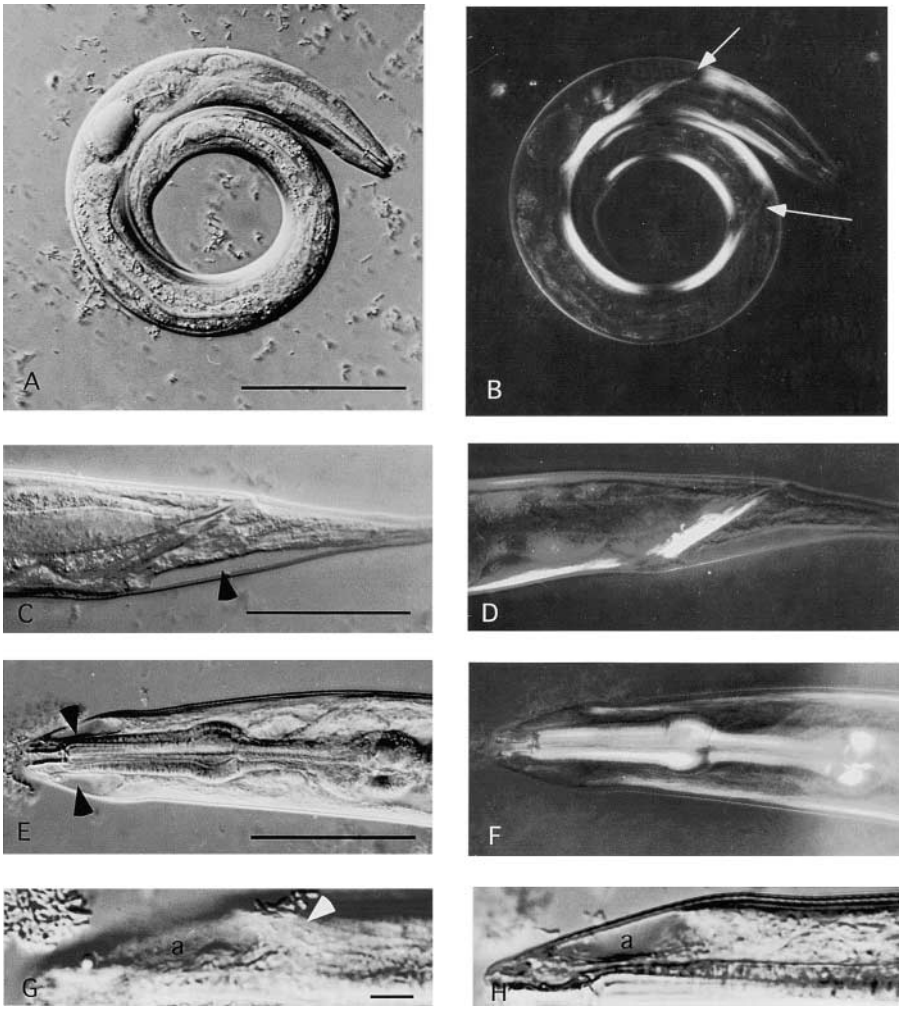

Figure 1. **DIC and polarized light micrographs of *mua-3* animals.** (A) DIC micrograph of a *mua-3(rh169)* animal showing typical curled posture. (B) Same animal as in A visualized by polarized light, a muscle band that has detached from the ventral body wall is visible as a bright birefringent band (arrows) that has collapsed dorsally. (C) DIC micrograph of *mua-3(rh195)* homozygote showing localized separation of tissues from the cuticle at tail (arrowhead). (D) Same as C under polarized light showing separation of ventral body wall muscles from tip of tail. (E) DIC micrograph of *mua-3(rh195)* homozygote showing localized separation of tissues from cuticle in head region (arrowheads). (F) Same as C under polarized light showing rearward retraction of the body wall muscles from the area of tissue separation. (G and H) Enlargements of area of tissue separation, two different focal planes of same animal as in E. Note retracted muscles (arrowhead in G) about the region of separation. The large blister labeled a appears to due to separation of the apical hypodermal membrane from the cuticle. Bars: (A–F) 100 μm; (G and H) 10 μm.

moter, rescues (data not shown). Consistent with the identification of this gene as *mua-3*, RNA interference (Fire et al., 1998) using *mua-3* sequence results in a severe muscle detachment phenotype indistinguishable from strong *mua-3* alleles (see Hong et al., 2001, in this issue).

Reverse transcription (RT)-PCR using primer sequences from the predicted *mua-3* open reading frames was used to generate a complete *mua-3* splice leader 1 (SL1)-spliced cDNA (Fig. 3 A; EMBL/GenBank/DDBJ accession no. AAD29428). The cDNA sequence confirmed the majority of the predicted exon–intron boundaries with minor splice site and resultant reading frame corrections, and demonstrated that open reading frames originally assigned by GENEFINDER (The *Caenorhabditis elegans* Sequencing Consortium, 1998) to predicted proteins K08E5.3 and T20G5.3 are part of a single transcription unit.

The predicted MUA-3 protein is 3,767 amino acids long and composed of a large extracellular domain that includes 5 low density lipoprotein type A (LA), 52 EGF, 1 von Willebrand factor type A (VA) and 2 sea urchin-agrin-enterokinase (SE) modules, a single transmembrane helix, and a 328 amino acid cytoplasmic domain (Fig. 3 B). The cytoplasmic domain does not contain recognizable protein modules. BLAST searches of the databanks using complete or partial MUA-3 amino acid sequence revealed a closely related *C. elegans* gene 2 megabases distant from *mua-3* on chromosome III. The *C. elegans* homologue has been subsequently shown to encode the tissue fragility gene *mup-4* (Gatewood and Bucher, 1997; Hong et al., 2001). MUP-4 contains no LA and fewer EGF modules than MUA-3, but shows 50% amino acid sequence identity with MUA-3 in the shared portions of the extracellular domain. The cytoplasmic domains of MUA-3 and MUP-4 are less similar: the MUP-4 cytoplasmic is shorter (223 amino acids versus 328 for MUA-3), and has only 37% identity in the shared region, much of it due to compositional bias rather than conserved primary sequence. Database searches also identified the partial genomic sequence of an *mua-3* orthologue in the sister species *C. briggsae* on cosmid MM14H7 (Washington University Genome Sequencing Center, *C. briggsae* sequence project). This sequence starts within the coding region of the fourth EGF module. The partial cbMUA-3 is virtually identical with MUA-3, showing 95% sequence identity in the extracellular domain and 84% identity in the cytoplasmic domain. No nonnematode orthologues were identified.

The MUA-3 calcium-binding EGF (EC) and LA modules are novel variants

The EGF and low density lipoprotein A (LA) modules that are found in MUA-3 are novel varieties (Tables I and II).

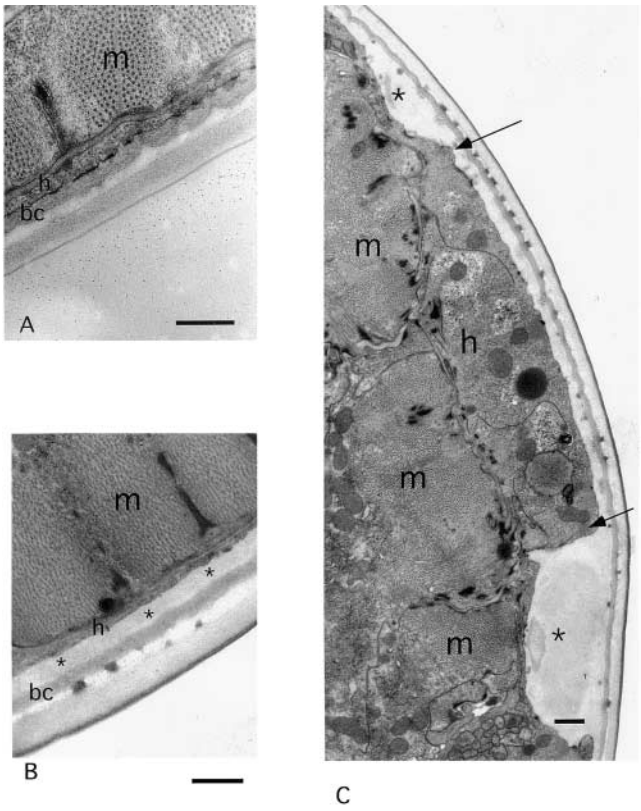

Figure 2. ***mua-3* is required for attachment between the apical hypodermal surface and cuticle.** (A and B) TEM micrographs of adult wild-type and *mua-3(rh195)* body wall in intact muscle quadrants. Body wall muscle is indicated by m, hypodermis h, and the basal layer of the cuticle by bc. In the mutant an obviously substantial gap (asterisk) between apical hypodermis and cuticle can be observed. (C) TEM micrograph of *rh195* mutant body wall in region of muscle detachment. Large gaps indicated by (asterisk) are observed between apical hypodermis and basal cuticle. Hypodermis (h) remains tightly apposed to muscle (m) in the detachment region. A portion of the hypodermis (region between arrows) has become decompressed in the detachment region, whereas immediately under the gaps it is still compressed. Bars, 0.5 μm.

The LA modules contain only four of the six conserved cysteines found in classical LA modules, but otherwise retain all conserved residues implicated in ligand binding (Russell et al., 1989). The EGF modules are most closely related to the Ca^{2+} binding class (EC), but 37 contain a novel 8–10-residue insert that may form an extended Ω-loop, and show an unusual pattern of potential metal binding residues (aspartate and asparagine), suggesting that this loop plays a role in forming intermodule coordination contacts (Handford et al., 1991). A search of the databanks showed only one nonnematode example of this novel form of EC module in a 63-kD sea urchin sperm membrane protein (Mendoza et al., 1993).

MUA-3 is localized in hypodermal cells at sites of body wall muscle adhesion

The structure and phenotype of MUA-3, together with previous genetic evidence that indicated *mua-3* activity has a hypodermal focus (Bucher and Greenwald, 1991; Plenefisch et al., 2000), suggested that MUA-3 might localize to hypodermal hemidesmosomes. Monoclonal antibodies were raised to the COOH-terminal 84 amino acids of the cytoplasmic domain, a region with no significant amino acid homology to any other *C. elegans* protein, including MUP-4. Three independent anti–MUA-3 monoclonal antibodies were obtained and used to localize MUA-3 in fixed specimens by indirect immunofluorescence (Miller and Shakes, 1995). The major site of MUA-3 localization is the hypodermis at the sites of muscle contact (Fig. 4). The immunofluorescence coincides with the extent of the body wall muscle bands and shows a repeating pattern of closely spaced circumferential stripes (~0.4 μm periodicity) separated by an unstained gap (~0.2 μm) in adults. Individual stripes are not uniformly stained, but rather composed of many individual spots and frequently contain a narrow central nonstaining region. Where neuronal processes interpose between hypodermis and basal lamina, MUA-3 is absent, resulting in stereotypical gaps (Fig. 4). The MUA-3 localization pattern is virtually identical with those reported for MH4 and p70 (IF proteins) and MH46 (myotactin) (Francis and Waterston, 1991; Hresko et al., 1999). During embryogenesis, MUA-3 is observed in twofold and older embryos (e.g., Fig. 6 E).

MUA-3 also localizes to sites where other striated muscles make adhesive contact and transmit force across the hypodermis. These include the vulval muscles (not shown), the anal depressor muscle, and the junctions between anal sphincter muscle and rectal cuticle that cross the intestinal/rectal epithelium (Fig. 5; White, 1988).

MUA-3 localizes to several sites where nonmuscle cells make tight transhypodermal contacts to the cuticle (Fig. 5). It is present in thin longitudinal stripes where the touch neurons (ALM and PLM) compress the hypodermis to make close contact with the cuticle, and where the sensory dendrites of the amphid, phasmid, and IL neurons penetrate the hypodermis and cuticle to form externally exposed sensilla (Chalfie and Sulston, 1981; Perkins et al., 1986). MUA-3 also localizes to the excretory duct and pore cells, both of which contain a cuticle lined lumen (Nelson et al., 1983). Finally, MUA-3 was not detected at the uterine seam, where the uterus makes indirect IF mediated contact to the cuticle via the seam cells (White, 1988; unpublished data), or in the pharynx, where IF bundles link the basal lamina to the lumenal cuticle (White, 1988; Francis and Waterston, 1991).

MUA-3 colocalizes with hypodermally expressed IFs but does not organize them

To determine if the MUA-3 localization pattern at the sites of body wall muscle contact could be the result of direct interactions between MUA-3 and hypodermal hemidesmosomes, we examined the immunofluorescent localization of MUA-3 in animals also labeled with anti-p70, a rabbit polyclonal antibody that recognizes cytoplasmic IFs associated with the hypodermal hemidesmosomes (Francis and Waterston, 1991). Both p70 and MUA-3 localize to the same circumferential stripes within the hypodermis at the sites of body wall muscle contact, showing that MUA-3 is localizing to the hemidesmosomes, rather than the regions between them (Fig. 6, A–C). This colocalization is apparent in embryos from the twofold stage in Fig. 6, D–F. IFs are also

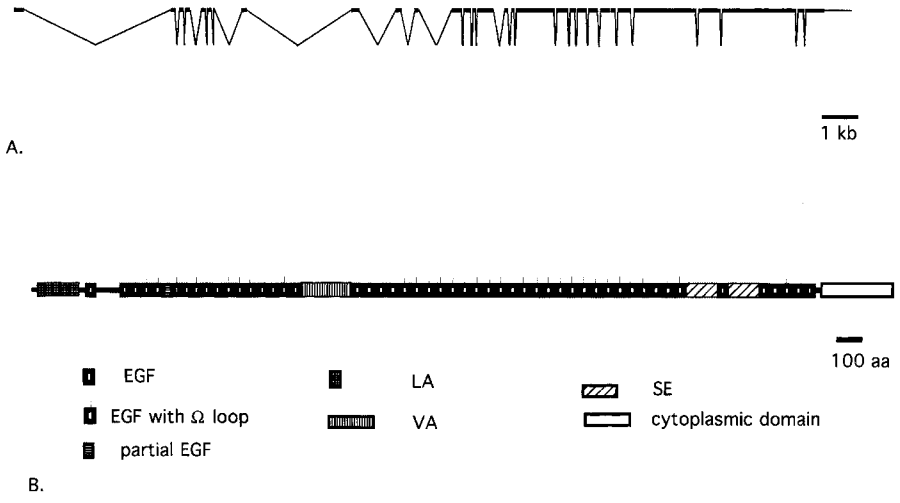

Figure 3. **Structures RNA and protein from *mua-3* gene.** (A) RNA transcript structure as determined from RT-PCR–generated cDNA (EMBL/GenBank/DDBJ accession no. AAD29428). The relative positions and sizes of exons are shown, and the splicing joins are indicated by Vs. The 5′ end transsplices to SL1. (B) The domain/module structure of the MUA-3 protein as deduced from the predicted amino acid sequence. The two letter module labels conform to those used in Hutter et al., (2000), see footnotes.

consistently present at or adjacent to other sites of MUA-3 localization, including the touch neurons, rectum, excretory duct, and pore (Fig. 6, G–I). The double localization studies also provide additional evidence that MUA-3 localizes to the apical, cuticle-facing surface of epithelial cells; MUA-3 staining was seen to be more lumenal than p70 in the duct and pore cells of several specimens (Fig. 6, G–I).

Animals mutant for *mua-3* were stained with anti-MUA-3, anti-p70, and MH5, an antibody that recognizes a non-IF hemidesmosome–associated antigen (Francis and Waterston, 1991). In the nonnull *rh169* and *rh195* mutants, MUA-3 no longer localizes to the hypodermal hemidesmosomes, but rather appears to be diffusely staining throughout the hypodermis (Fig. 7 A). However, these same mutations did not result in disruption of IF organization in the hypodermis (Fig. 7 B). In *mua-3* animals, MH5 is also normally organized in regions where muscle detachment has not occurred (Fig. 7 F). However, where muscles have detached, MH5 staining is lost from the body wall and can be seen associated with the detached muscle, consistent with separation between the apical hypodermal surface and cuticle (Fig. 7, C–E). These results suggest that IFs may help to localize MUA-3, but also that MUA-3 is not required for IF localization or hemidesmosome assembly.

Discussion

In *C. elegans*, two classes of genes required for the normal attachment of muscles to the cuticle via basal lamina and hypodermis have been described. Mutations that prevent or perturb assembly of the mechanical links between muscle and cuticle by deleting major structural proteins within them have been shown to result in an embryonic paralysis (Williams and Waterston, 1994; Hresko et al., 1999). Other mutations in genes distinct from those of the first class result in a progressive flaccid paralysis due to use-dependent failure of apparently normally assembled structures (Plenefisch et al., 2000). Here we have demonstrated that one of these latter genes, *mua-3*, encodes a transmembrane protein that colocalizes with IFs at hypodermal hemidesmosomes and other sites where stress is transmitted from epithelial cells to cuticle, and that MUA-3 functions at the hypodermal–cuticle interface.

Table I. **Sequence comparison of classical and MUA-3–truncated LA modules**

	1 2 3 4 5 6
LDL-receptor:LA3	CSQ-DEFRCH-DGKCISRQFVCDSDRDCLDGSDEASCPVLT-
UNC-52 perlecan:LA1	CGP-QEASCH-SGHCIPRDYLCDGQEDCRDGSDELGCASPPP
MUA-3:LA1	CVAREEFQCKMDDSCISMKKWQDGVDDCYDGSDEV-------
C. elegans MUP-4	CPP-NTFTCA-DGSCIPSDWKGDGEKDCEDGSDEE-------
consensus	C F C CI D DC DGSDE

Table II. **Sequence comparison of classical and MUA-3 modules**

	47 50 64
factor IX:EC1	DGDQCES---NPCLNGGSCKDDINSYECWCPFGF----------EGKNCEL
fibrillin:EC	DIDECQR-DPLLCR-GGVCHNTEGSYRCECPPGH-QLSP-----NISACI
Notch:EC	DIDECQS---NPCLNDGTCHDKINGFKCSCALGF----------TGARCQI
Notch:EC	DIDECDQ--GSPCEHNGICVNTPGSYRCNCSQGF----------TGPRCET
sperm 63-kD:EC2	DFDECASADDNDCDPNANCTNTAGSFTCECDTELYDNSPNTEE-PGRVCIA
MUA-3:EC5	AINECAS-NLHNCDTHAICQDQPVGYSCRCPFGFIDSSPTALE-PGRKCVQ
MUA-3:EC37	LVDECRE-GRHTCSSHADCRDLEEGYTCECRDGYVDRSPNLASQPGRVCSA
MUA-3:EC42	LINECLDRSLNDCHSLAVCKDLPNGYTCQCPINAKDQSPDPRK-PGRICSL
MUA-3:ECconsensus	NEC C A C D GY C C D S PGR C

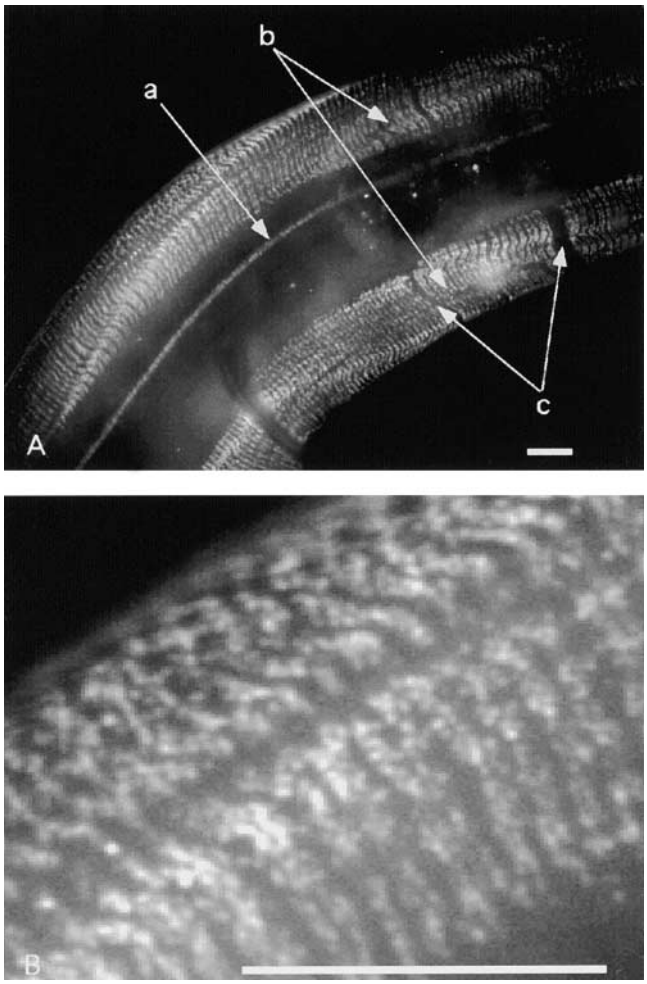

Figure 4. **Localization of MUA-3 to hemidesmosome zone of hypodermis in animals stained with anti–MUA-3 antibodies.** (A) Immunofluorescence in hypodermis-bordering muscle quadrants using MUA-3 antibody recognized with a FITC secondary antibody. a, ALM; b, hemidesmosome region of hypodermis; c, gaps where nerve processes cross between hypodermis and muscle. (B) Enlargement of hemidesmosome region of hypodermis. Bars, 10 μm.

MUA-3 is a novel transmembrane receptor protein

MUA-3 is a predicted 3,767 amino acid single pass transmembrane protein. The extracellular domain consists of four distinct protein modules, 5 LA, 52 EGF, 1 VA, and 2 SE modules (Fig. 3). Expressed at the apical hypodermal surface, MUA-3 could penetrate as far as the fibrous layers of the adult cuticle. Individual EGF modules are ~3 nm by 2 nm; 52 EGF modules could extend up to 150 nm in an extended conformation (Downing et al., 1996). In a folded conformation, the EGF rod would still be expected to extend >50 nm. Since non-EGF modules also contribute to MUA-3's overall size, these numbers are minimum estimates for the length of the extracellular domain. The adult *C. elegans* cuticle is a multilayer structure, the basal layer of the cuticle is closely apposed to the apical hypodermal surface and ~100–150 nm in thickness (Fig. 2 A; Kramer, 1997; Peixoto et al., 1998). Fibers extending up to 100 nm into this layer from the apical hemidesmosomes can be seen in electron micrographs (Francis and Waterston, 1991; Peixoto et al., 1998).

The EC and LA modules found in MUA-3 are novel varieties (Tables I and II). Despite their shorter size and lack of cysteines 4 and 6, we predict no major alterations in the overall structure of the LA module and they retain all conserved residues implicated in ligand binding (Russell et al., 1989). Furthermore, an examination of LA modules found in the *C. elegans* matrix and cell receptor proteins shows that although most *C. elegans* LA modules contain the canonical six cysteines, several proteins contain the shorter form (Hutter et al., 2000). Whether this form is nematode-specific is not yet known. One possibility is that the short LA modules are adapted to bind specific molecules found in the nematode cuticle.

The MUA-3 EC modules contain a novel 8–10-residue Ω-loop inserted at position 77 of the canonical sequence, and show an altered pattern of potential metal binding residues (Handford et al., 1991). In canonical EC modules, Ca^{2+} is coordinated by aspartate at positions 47 and 49 together with aspartate or asparagine at position 64. In MUA-3, aspartate is not present at position 47, instead a conserved aspartate is located at position 2 of the Ω-loop. We suggest that the Ω-loop and altered positions of the putative metal binding residues may allow for Ca^{2+} ions to be coordinated between adjacent EC modules in MUA-3. With Ca^{2+} bound, the EC rod may adopt a compacted form, when Ca^{2+} is released, an extended form. Thus, MUA-3 could have mechanical properties similar to a spring, maintaining cuticle attachment as new cuticle forms and displaces older cuticle outwards, despite bending and stretching of the mechanical path. Database searches identified only three other genes that contained this EC variant: MUP-4 from *C. elegans*, the MUA-3 orthologue from *C. briggsae*, and a 63-kD sea urchin sperm membrane protein (Swiss-Prot spQ07929). The protein sequence between EGF modules five and six appear to be a degenerate EGF module that lacks the first and second cysteines.

MUA-3 contains a single VA module. These have been shown to bind fibrillar-type collagens in other systems (Colombatti and Bonaldo, 1991); by analogy, the VA module in the center of MUA-3 may be binding to cuticle collagens. MUA-3 also contains two SE repeats, these are modules of unknown function associated with O-glycosylation found in several extracellular matrix proteins, including perlecan, agrin, and the 63-kD sea urchin sperm protein noted above (Bork and Patty, 1995).

The MUA-3 cytoplasmic tail, while not directly homologous to any known protein, has the amino acid compositional bias seen in filaggrins, proteins known to bind to IFs (Mack et al., 1993). Although alone this bias is only weakly suggestive, the observation that MUA-3 colocalizes with cytoplasmic IFs suggests MUA-3 may directly bind IFs.

Two MUA-3 homologues, both in nematodes, have been identified. One is the *C. elegans* MUP-4 protein that contains fewer EC repeats and lacks the LA modules of *mua-3* (Hong et al., 2001). The second is an orthologue from the related nematode species, *C. briggsae*, that shows >90% identity throughout the coding region. Unambiguous orthologues have not been identified to date in nonnematodes. This could be because this protein family is nematode specific, or because they are highly diverged in different phyla.

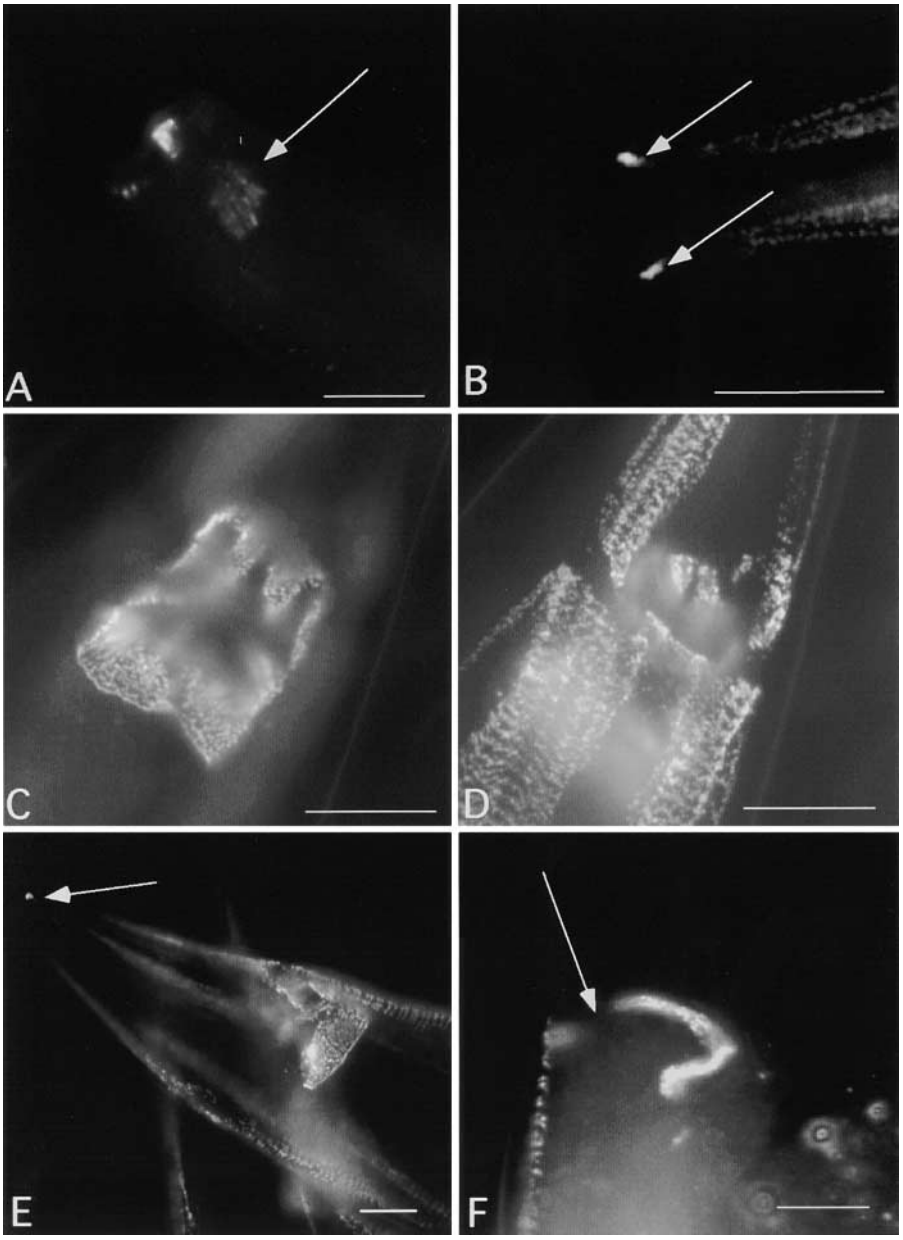

Figure 5. **Localization of MUA-3 to nonmuscle body wall muscle sites.** (A) Amphids, indicated by arrow. (B) Phasmid sensilla in tail (arrow). (C and D) Rectum, shown in two focal planes, posterior to upper right. The staining forms a collar completely surrounding the rectal valve, where the sphincter muscle sits. Hypodermis bordering body wall muscle can also be seen in D. (E) Side view rectum, again note collar of staining surrounding rectal valve. Arrow indicates phasmid. (F) The excretory duct cell and pore cells. Arrow indicates consistent gap in MUA-3 pattern seen at pore cell/duct cell boundary. Bars, 10 μm.

MUA-3 localizes to sites of transhypodermal stress

MUA-3 localizes to sites where transepidermal mechanical attachments are formed between nonepidermal cells and cuticle; these include striated muscles, neurons, and several other cells that interface directly with the hypodermis (White, 1988). IFs are also present at all these sites (Francis and Waterston, 1991; Fig. 6 and unpublished data).

MUA-3 localizes to hemidesmosomes where hypodermis contacts body wall muscle, a localization that is shared with several other hypodermally expressed proteins implicated in muscle force transmission. These include myotactin, IFs, and MUP-4 (Francis and Waterston, 1991; Hresko et al., 1999; Hong et al., 2001). MUA-3 expression is observed as early as at the twofold stage, a stage at which muscle function is first required in the developing embryo (Barstead and Waterston, 1991; Hresko et al., 1994).

MUA-3 also localizes to the hypodermal attachment sites of the vulval and anal depressor muscles. In addition, MUA-3 is found where the sphincter muscle makes force-transmitting linkages to the rectal cuticle. The sphincter muscle formed a torroid surrounding the rectal epithelial cells and separated from them by basal lamina; its contraction and relaxation are used to control the flow of wastes through rectal valve (White, 1988). Although the ultrastructure of cellular attachments in this region is not well described, the sphincter muscle must transmit force to the rectal cuticle via the interposed epithelium.

MUA-3 is found at several sites where sensory neuronal processes make contact with or penetrate the cuticle. The mechanosensory processes of the ALM and PLM neurons run longitudinally along the body wall in deep hypodermal clefts and make close mechanical contact to the cuticle (Chalfie and Sulston, 1981). A localized matrix, the mantle, surrounds the process, and hemidesmosome-like plaques and IFs have been visualized in the thin layer of hypodermis between the mantle and cuticle (Chalfie and Sulston, 1981;

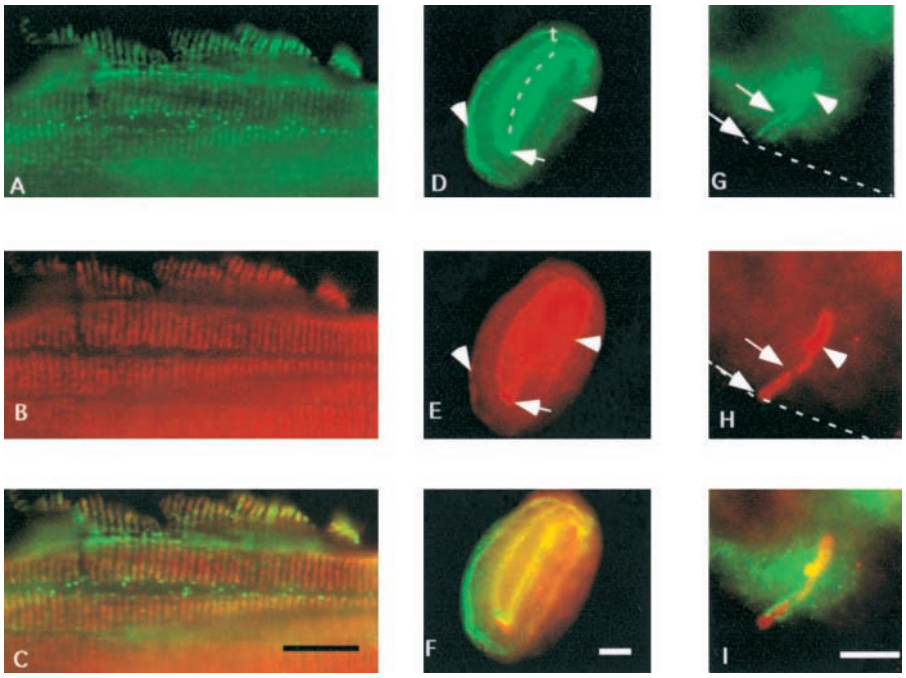

Figure 6. **MUA-3 colocalizes with cytoplasmic IFs at hypodermal hemidesmosomes.** It is also associated with MUA-3 at other sites of MUA-3 localization in animals double stained with anti-p70 (IF) and MUA-3 antibodies. (A) IFs associated with hypodermal hemidesmosomes visualized with anti-p70 in an adult. (B) Same animal stained for MUA-3. (C) Merge of A and B. (D) p70 localization in threefold embryo. Embryo is folded on itself: t indicates location of tail; the dashed line shows location of fold between posterior and central body regions, the anterior region is folded under the posterior end and not in field of view. Ventral- and dorsal-staining stripes in hypodermis are visible and indicated by arrowheads and an arrow, respectively. (E) Same embryo showing MUA-3 localization. Note stripe pattern similar to p70, indicated by arrowheads and an arrow. (F) Merge of E and F. (G) Duct and pore cells showing p70 IF localization. Ventral is down, dashed line indicates location of body wall (not visible), arrows indicate pore cell (note lack of staining in hollow lumen), and the arrowhead indicates the duct cell. (H) Same, showing MUA-3 localization. Note that MUA-3 is located closer to the lumenal cuticle and extends closer to body wall than the p70, especially apparent in the pore cell (arrows). Arrowhead indicates duct cell. (I) Merge of G and H. Bars, 10 μm.

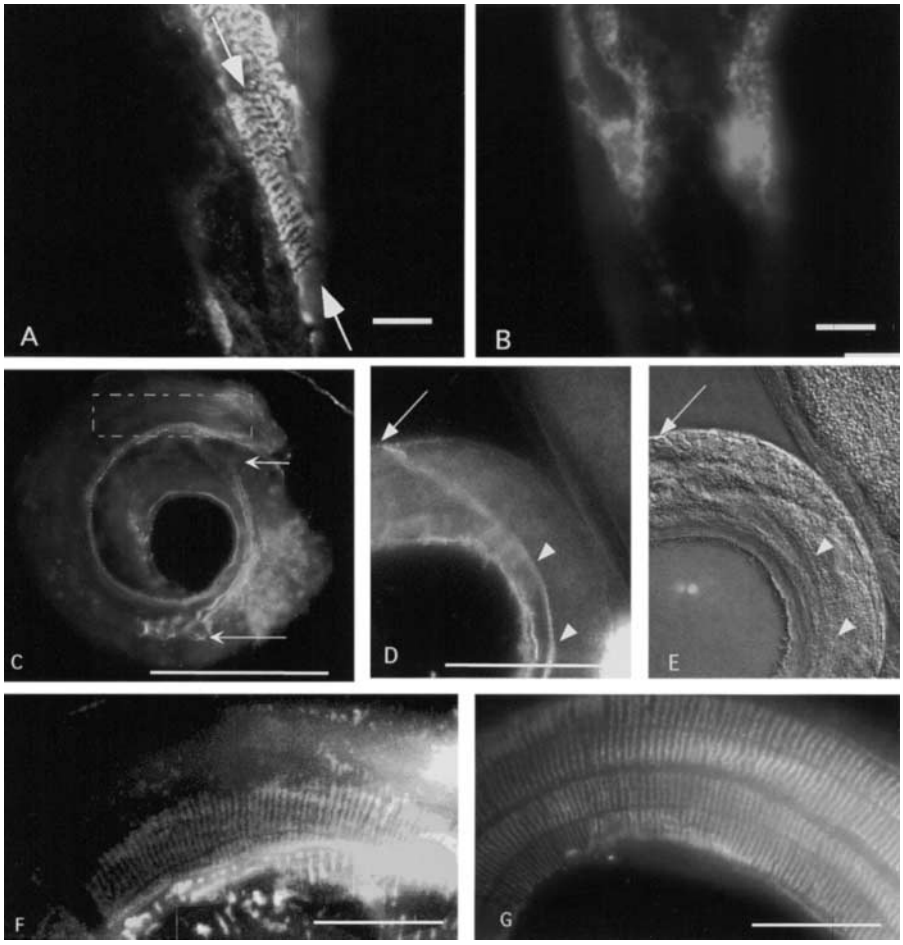

Figure 7. **In *mua-3* mutants hemidesmosomes show normal assembly and patterning.** (A and B) L4 stage *mua-3(rh169)* doubly labeled for IFs (p70) (A) and MUA-3 (B). Note presence of organized IFs (between arrows), despite disorganized MUA-3 localization. (C) L2 stage *mua-3(rh169)* stained with hemidesmosomal marker MH5. Arrows indicate region of separation of MH5 staining from the cuticle. Dotted rectangle indicates area of enlargement in D. (D) Different *mua-3(rh169)* animal also stained with MH5. MH5 staining separates from cuticle at arrowhead and runs through interior of animal (arrowheads). (E) Same animal as in E under DIC illumination shows muscle, visible as detached band (arrowheads), separating from body wall at arrow. Note that MH5 in E localizes with the muscle, suggesting that the basal hypodermis remains attached to the musculature. (F) Same animal as D, enlarged view of area indicated in C showing that MH5 localization is normal where muscles remain attached to the body wall. (G) Age-matched wild-type animal, showing normal MH5 pattern Bars: (A–E) 10 μm; (F and G) 1 μm.

Francis and Waterston, 1991). MUA-3 is present along the entire length of the touch neuron attachment zone. MUA-3 is also detected where the amphid, phasmid, and interlabial sensilla penetrate the cuticle. In these sites, two nonneuronal cells completely surround the neuronal processes, forming a channel through which ciliated neuronal endings are exposed to the external environment (Perkins et al., 1986). The socket cell's channel is cuticle lined. This cell forms adherens contacts to itself, the hypodermis, and the underlying sheath cell. The sheath cell's channel is filled with copious amounts of an undefined electron-dense matrix material, and a filamentous scaffold of IFs is found in its cytoplasm (Perkins et al., 1986). MUA-3 appears to localize to the socket cell (which makes cuticular and hypodermal contact) and not the sheath cell (which does not) (Fig. 6).

MUA-3 is found at the cuticle-facing surface of the excretory system's duct and pore cells. These two cells connect the lumen of the excretory canal to the external environment (Nelson et al., 1983). The pore cell interfaces directly with the hypodermis and the duct cell connects the pore and excretory cells. The apical lumen of both duct and pore is cuticle lined and IFs are found in their cytoplasms. The basal surfaces face a basal lamina continuous with that separating the muscles from the hypodermis; however, there is no evidence to suggest they form adhesions to the muscle cells.

A model for MUA-3 function

The available evidence suggests that MUA-3 is only, or primarily, found at junctions between epithelial IFs and cuticle. TEM shows that the initial MUA-3 defect involves attachment between the apical hypodermal surface and the cuticle (Fig. 2), MUA-3 localizes apically at the duct and pore cells (Fig. 6), and, at all sites where MUA-3 has been shown to localize, cuticle is present.

We propose that MUA-3 binds IFs through its cytoplasmic domain and cuticle via its extracellular domain. Furthermore, the extracellular domain is predicted to be a flexible tether accommodating movement and growth while maintaining attachment strength. MUA-3 may also act to signal growth or stress, resulting in the recruitment of additional IFs and other unidentified receptor proteins to the stress sites. In particular, sites where muscle force is transmitted across the hypodermis are dependent on MUA-3 function: when MUA-3 activity is reduced or lost these sites fail, resulting in separation of the musculature from the body wall. In *mua-3* mutants, muscles peel from the body wall as an intact band with concomitant decompression of the hypodermis in the region of detachment. This muscle detachment and hypodermal decompression are likely a secondary consequence of hypodermal-cuticle attachment failure. In mutants, the gap between the apical hypodermis and the basal cuticular layer appears enlarged before detachment, this gap enlarges as detachment initiates (Figs. 1 and 2). As the muscles collapse away from the body wall the hypodermal basal surface remains attached to the muscles, and compression of the hypodermis at the sites of muscle detachment is lost. In the strongest alleles, the muscles eventually collapse to the opposite side of the animal as it becomes locked in a bent posture and the hypodermis appears to herniate once the force of muscle contraction is no longer transmitted to cuticle, but is instead absorbed by the hypodermis, and the animals typically die (Plenefisch, et al., 2000). Thus, the gross phenotype of *mua-3* is proposed to result from compromised attachments between hypodermis and cuticle with resulting separation of these two layers in response to muscle use as the initiating event.

No phenotype associated with the loss or reduction of MUA-3 activity at other cellular sites has been yet unambiguously observed. Since previous studies have shown that the penetrance of muscle detachment in *mua-3* animals is use-dependent (Plenefisch et al., 2000), one possibility is that only sites with the greatest stress (i.e., those associated with the skeletal muscles) will show obvious tissue damage. In addition, since no alleles have been shown to be a definitive null, other MUA-3 functions cannot be ruled out, including possible roles for MUA-3 at the basal hypodermal surface.

The MUA-3 protein is not required for the initial assembly of the hypodermal hemidesmosomes: IF arrangement looks relatively normal in mutant animals and phenotypic onset is postembryonic (Fig. 7 and unpublished data). Unlike MUA-3, myotactin has been shown to localize to the basal hypodermal surface and may play a direct role in the initial assembly. In myotactin mutants, IFs are not localized to the regions of body wall muscle apposition and muscle detachment occurs embryonically (Hresko et al., 1999). MUP-4 appears to be required for embryonic attachment of hypodermis to cuticle, *mup-4* mutants result in an embryonic arrest, muscles are invariable mispositioned, detached or disorganized, and the hypodermis itself is often abnormally organized with apparent lack of adhesion between apical hypodermal surface and cuticle (Gatewood and Bucher, 1997; Hong et al., 2001). Thus, both myotactin and MUP-4 are candidates for controlling the embryonic organization of hemidesmosomes, whereas MUA-3 is required for the maintenance of these attachment sites postembryonically.

C. elegans and vertebrate hemidesmosomes: convergent evolution?

The hypodermal hemidesmosomes of *C. elegans* are ultrastructurally similar to vertebrate type I hemidesmosomes. The vertebrate type I hemidesmosomes have electron-dense membrane-associated plaques from which IFs extend into the cytoplasm, and a subbasal plaque from which anchoring fibrils extend into the lamina densa are observed (for review see Nievers et al., 1999). The cytoplasmic plaques are associated with HD1/plectin, BP230, $\alpha4\beta6$ integrin, and BP180. The latter two molecules are transmembrane receptors that promote adhesion of the epithelium to the basal lamina, with $\alpha4\beta6$ integrin binding laminin type 5. *C. elegans* hemidesmosomes contain dense plaques at the cell membrane, into which cytoplasmic tonofilaments can be observed inserting, and from which fibrils extend into the surrounding matrix (Francis and Waterston, 1991). Molecules associated with these nematode hemidesmosomes include cytoplasmic IFs, myotactin, MUP-4 and MUA-3, and the uncharacterized MH5 (Francis and Waterston, 1991; Hresko et al., 1999; Hong et al., 2001). Interestingly, $\alpha4$ or $\beta6$ integrin orthologues are not present in the nematode genome, and reported mutations in the known nematode integrins do not affect hypodermal structures (Williams and

Waterston, 1994; Baum and Garriga, 1997; Hutter et al., 2000). In addition, although the genome contains plectin, no obvious BP230 or BP180 orthologues are present (Hutter et al., 2000). Conversely, no vertebrate orthologues of myotactin, MUP-4, and MUA-3 have been identified. One intriguing possibility is that these are nematode-specific proteins that substitute for integrins and BP180 in nematode hemidesmosomes.

Why might nematode and vertebrate hemidesmosomes utilize such different matrix receptors? One possibility is that the hemidesmosomes of vertebrates and invertebrates are evolutionarily convergent structures. In support of this possibility is the observation that nematode cytoplasmic IFs are more closely related to nuclear lamins than to vertebrate cytoplasmic IFs, e.g., the cytoplasmic IFs of nematodes and vertebrates are not orthologous (Dodemont et al., 1994). In addition, the hemidesmosomes of the nematode hypodermis make adhesive links to two dissimilar types of matrix. The basal lamina is similar, but not identical, to vertebrate basal lamina (Kramer, 1997; Hutter et al., 2000) and presumably cells could bind via the same types of matrix receptors. The nematode cuticle is structurally and compositionally unique and would presumably require novel matrix receptors (Kramer, 1997). In *C. elegans* specialized receptors such as MUA-3 that bind to the cuticle, myotactin that binds to the nematode basal lamina, or other receptors that have the capacity to bind both matrices, may have been preferentially selected for and retained in the genome, whereas β4-type integrins or BP180-like receptors either never evolved or were lost in nematodes. Clearly a comparative genomic approach is required to resolve this issue; in this respect it is intriguing to note that the *Drosophila* genome does not contain genes encoding hemidesmosomal components, cytoplasmic IFs, or nematode or vertebrate-type hemidesmosome matrix receptors (Tepass and Hartenstein, 1993; Rubin et al., 2000; unpublished data).

Materials and methods

Strains, culture, and DIC observation

Methods for routine culture, genetic manipulation, and microscopic observation of live *C. elegans* are described in Epstein and Shakes (1995). The sources of the *mua-3* alleles are given in Plenefisch et al. (2000); *ju135* was a gift from Andrew Chisholm (University of California, Santa Cruz, CA). Other mutations used in this study, described in Riddle et al. (1997), are *ced-7(n1892)* III, *unc-32 (e189)* III, *unc-69(e587)* III, and *rol-6(su1006sd)*. The balancer chromosome *qC1* is described in Edgley et al. (1995). Differential interference contrast (DIC) and polarized light micrographs were taken using Technical Pan Film at ASA 125 (Eastman Kodak Co.) and developed in HC110 dilution B (Eastman Kodak Co.) for 9 min at 20°C. Determination of the sites and timing of muscle detachment were as described in Plenefisch et al. (2000).

Electron microscopy

Animals were embedded and stained based on the protocols of Hall (1995), with the exception that 0.5% $K_3Fe(CN)_6$ was added to the OsO_4 staining reagent. Poly/Bed 812 from the Poly/Bed 812 BDMA Mini-Kit (Polysciences, Inc.) was used as the embedding medium.

Positional cloning of MUA-3

The *mua-3* gene was positioned between *ced-7* and *unc-69* (Fig. 8). *ced-7++/+mua-3 dpy-18* and *unc-32+mua-3/+ced-7+* animals were generated and allowed to self. Dpy non-Mua and Unc non-Mua recombinants were picked and their progeny scored for Ced animals. 10/10 Dpy recombinants and 0/2 Unc recombinants segregated Ced, placing *ced-7* to the left of *mua-3*. Unc non-Dpy recombinants from *dpy-17+unc-69/+mua-3+* self-progeny were picked; 2 out of 21 segregated Mua, placing *unc-69* to the right of *mua-3*.

The genomic DNA sequence of the *ced-7* to *unc-69* interval (~800 kb) was searched for potential candidate's genes (The *Caenorhabditis elegans* Sequencing Consortium, 1998). Phenotype and mutation frequency suggested that MUA-3 should be a large transmembrane protein containing matrix-associated modules. A matching candidate was identified, it corresponds to GENEFINDER predictions K08E5.3 and T20G5.3; the complete coding sequence is contained on cosmid F55E6. We obtained F55E6 and flanking cosmids from the Sanger Center, Hinxton, Cambridgeshire, UK. pOT22 is derived from F55E6 by XhoI partial digestion and religation; it contains 4.1 kb of the sequence upstream of the predicted start codon of *mua-3*, all open reading frames, and no other predicted genes. DNA was prepared and reintroduced into *unc-32(e189) mua-3(rh169)/qC1* animals using standard protocols described in Mello and Fire (1995) and coinjected with marker plasmid pRF4 containing *rol-6(su1006sd)*. Broods from injected animals were screened for rescued non-Mua Unc Rol progeny. In addition, Rol non-Unc animals were individually picked to separate plates and their progeny scored for non-Mua Unc Rol animals.

RT-RCR

RT-PCR was used to confirm the predicted *mua-3* transcript structure and estimate transcript complexity. Primers were designed across the predicted open reading frames (Table III). The 3′ and 5′ ends were amplified using oligo-dT and SL1 primers, respectively. RNA was isolated using Tri Reagent (Molecular Research Center, Inc.). Animals were collected in M9 buffer and mixed with sand, Tri reagent, and chloroform. The RNA in the aqueous phase was precipitated with isopropanol. Reverse transcription was done using the Stratagene RT-PCR kit (Stratagene). The resulting PCR products were sent to the Johns Hopkins Molecular Core facility for sequencing.

Generation of anti–MUA-3 antibodies

A fusion protein with the *E. coli* maltose binding protein fused to the COOH-terminal 84 amino acids of MUA-3 was produced by ligating an EcoR1-HindIII fragment containing the *mua-3* termination codon into the multicloning site of pMal (New England Biolabs, Inc.). This construct was transformed into competent *E. coli* and fusion protein obtained using New England Biolabs pMAL protein fusion and purification system (New England Biolabs, Inc.), except as follows. The bacterial crude extract was run over a column of cyanogen bromide–activated Sepharose beads (Amersham Pharmacia Biotech) conjugated to maltose binding protein antibodies and eluted with diethylamine. Fractions were visualized by SDS-PAGE

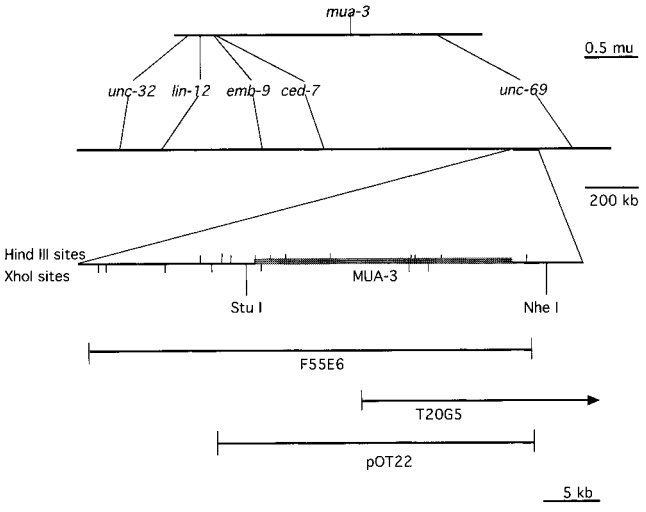

Figure 8. **Genetic (top) and physical (middle and bottom) maps of the *mua-3* region.** The vertical lines on the bottom map represent the location of restriction sites in the DNA sequence. The extents of F55E6, T20G5, and pOT22 relative to these sites are shown. The location of the open reading frames that comprise *mua-3* are shown as a gray bar. F55E6 and pOT22 rescue *mua-3* mutant animals, T20G5 does not.

Table III. **Primers used in RT-PCR**

MF(-45)	ATAGATGAGATTACTTTTTTTTGAC
MR307	CAAAATAGTGAGCAGGACAT
MF145	GATGGAGTTGATGATTGCTA
MF1067	CCGATGAAATAATAGACAGT
MR1112	TCGGGAGGTGTCATAATAGT
MF1516	AGAGAAGGAGCAAGAAAACC
MR2126	GACACAACAAACAGGATAGG
MF2094	TTTTACCAGAATGCCTATCC
MR2391	GTCCGAACTCTCATCTCTAT
MF3031	CCTGTTGAGAAGATAAAGAC
MR3066	AGTGTCCTTCAAATCAGTCT
MR3994	TATCACTCTGTTGCGGTCTT
MF3975	AAGACCGCAACAGAGTGATA
MF4820	ACGAATGTCTAACGGGTGAG
MR5085	TTGAGGATTTGGTGAGTAGT
MR5718	TTTTCTTCCGAGTCGGGTAA
MF5684	TTTCATTCGACAGAGTTACC
MF6679	GATAAGGAAGAAGGATACGA
MR6810	GTCGCAGTCGTTGAGTCTTG
MR7532	CGTGGTGGTGGAGATGGTGG
MF7500	CGAACCACCCCCACCACCAT
MF8511	TGATTGTATAAAGGCGAGAG
MR8573	CCTGGTTTACATCCGCAATA
MR9518	GGATCTGGTTGAGTTGGGTT
MF9449	ACGTCACCAAGGAAAATAAC
MF10525	GGAAATACAGCAGAAGTTAG
MR10736	GTTGTCTTGATTTCCTTTGT
MR11330	GGGATAATTGAATTTGAAAA
MF9736	TACAAATGCGAATGCTTACC

stained with Coomassie blue. A major protein of the predicted molecular weight was observed and the positive fractions used to immunize mice.

Initial injections were given to 8-wk-old female Balb/C mice subcutaneously with 50 ug of antigen in complete Freund's adjuvant. Three boosts were given at 2 wk intervals with 50 ug of antigen intraperitoneally without adjuvant. After the final injection, mice were boosted an additional 2 d and killed the fourth day. Splenocytes were isolated by passage through a wire mesh and red blood cells were removed by incubation with red blood cell lysis buffer (Sigma-Aldrich) on ice for 10 min. Primary splenocytes were fused with the mouse myeloma cell line P3/NS1/1-Ag4-1 (American Type Culture Collection) in the presence of polyethylene glycol (molecular wt 1,300–1,600; American Type Culture Collection). The complete fusion was plated in 96-well plates and media containing aminopterin added the following day to eliminate unfused myeloma cells. Hybridoma supernatants were screened by Western blot analysis. Positive hybridomas were cloned by limiting dilution to isolate a clonal population of antibody producing cells. Hybridomas were maintained in HY media (Sigma-Aldrich) supplemented with 20% fetal bovine serum (Hyclone Laboratories).

Two lines of evidence suggest that the antibodies are specific for MUA-3. First, Western blots of whole worm protein extracts show that the antibodies recognize a difficult-to-extract protein of >250 kD (not shown). Secondly, in mutant animals the distribution of the protein recognized by the antibodies is consistently disorganized (see Results).

Generation and characterization of MH5 and anti-p70 are described by Francis and Waterston (1991).

Immunofluorescence microscopy

Antibody staining protocols were as described in Miller and Shakes (1995). Mixed stage animals were harvested and resuspended in 50 μl of M9 buffer. For anti-MUA-3 and anti-p70 the worms were freeze-cracked followed by methanol-acetone fixation. Freeze-cracked specimens were blocked with PBS plus 10% goat serum (Sigma-Aldrich) for 1 h at 20°C before primary antibody addition. For MH5, the whole mount fixation method was used. Secondary antibodies were FITC- or rhodamine-conjugated goat anti–mouse antibodies (Jackson ImmunoResearch Laboratories). For double labeling with anti-MUA-3 and anti-p70, a combination of rhodamine-conjugated goat anti–mouse and FITC-conjugated goat anti–rabbit secondary antibodies were applied. Fixed worms were mounted for observation in Vecta Shield mounting medium with DAPI (Vector Laboratories) and the specimens were examined by epifluorescence on a ZEISS Axiophot microscope. Digital pictures were taken using a Spot camera (Diagnostic Instruments) and processed using Adobe Photoshop® software running on a G3 Power Macintosh.

We would like to thank Elizabeth Bucher and Michelle Hresko for useful discussions and communicating unpublished data, Margaret Wheelock for use of her monoclonal antibody facilities, and Gloria Stephney for expert electron microscopy assistance.

Some nematode strains used in this work were provided by the *Caenorhabditis* Genetics Center, which is funded by the National Institutes of Health National Center for Research Resources (NCRR). This work was supported by grants from the Muscular Dystrophy Association of America (MDA) to E. Hall, National Institutes of Health Center grant NIH RR12596 (D. Hall), and the American Heart Association (AHA) to J.D. Plenefisch.

Submitted: 9 March 2001
Revised: 5 June 2001
Accepted: 12 June 2001

References

Barstead, R.J., and R.H. Waterston. 1991. Vinculin is essential for muscle function in the nematode. *J. Cell Biol*. 114:715–724.

Baum, P.D., and G. Garriga. 1997. Neuronal migrations and axon fasciculation are disrupted in *ina-1* integrin mutants. *Neuron.* 19:51–62.

Bork, P., and L. Patty. 1995. The SEA module: a new extracellular domain associated with *O*-glycosylation. *Prot. Sci.* 4:1421–1425.

Bucher, E.A., and I.S. Greenwald. 1991. A genetic mosaic screen of essential zygotic genes in *Caenorhabditis elegans. Genetics.* 128:281–292.

Campbell, K.P. 1995. Three muscular dystrophies: loss of cytoskeletal-extracellular matrix linkage. *Cell*. 80:675–679.

The *Caenorhabditis elegans* Sequencing Consortium. 1998. Genome sequence of the nematode *C. elegans*: a platform for investigating biology. *Science.* 282: 2012–2018.

Chalfie, M., and J. Sulston. 1981. Developmental genetics of the mechanosensory neurons of *Caenorhabditis elegans*. *Dev. Biol.* 82:358–370.

Colombatti, A., and P. Bonaldo. 1991. The superfamily of proteins with von Willebrand Factor type A-like domains: one theme common to components of extracellular matrix, hemostasis, cellular adhesion and defense mechanisms. *Blood.* 77:2305–2315.

Costa, M., W. Raich, C. Agbunag, B. Leung, J. Hardin, J.R. Priess. 1998. A putative catenin-cadherin system mediates morphogenesis of the *Caenorhabditis elegans* embryo. *J. Cell Biol.* 141:297–308.

Diaz, L.A., and G.J. Giudice. 2000. End of the century overview of skin blisters. *Arch. Dermatol.* 136:106–112.

Dodemont, H., D. Riemer, N. Ledger, and K. Weber. 1994. Eight genes and alternative RNA processing pathways generate an unexpectedly large diversity of cytoplasmic intermediate filament proteins in the nematode *Caenorhabditis elegans*. *EMBO J.* 13:2625–2638.

Downing, A.K., V. Knott, J.M. Werner, C.M. Cardy, I.D. Campbell, and P.A. Handford. 1996. Solution structure of a pair of calcium-binding epidermal growth factor-like domains: implications for the Marfan syndrome and other genetic disorders. *Cell.* 85:597–605.

Edgley, M.L., D.L. Baillie, D.L. Riddle, and A.M. Rose. 1995. Genetic balancers. *In Caenorhabditis elegans*: Modern Biological Analysis of an Organism. H.F. Epstein and D.C. Shakes, editors. Academic Press, San Diego, CA. 147–184.

Epstein, H.F., and Shakes, D.C., editors. 1995. *Caenorhabditis elegans*: Modern Biological Analysis of an Organism. Academic Press, San Diego, CA. 659 pp.

Fire, A., S. Xu, M.K. Montgomery, S.A. Kostas, S.E. Driver, and C.C. Mello. 1998. Potent and specific genetic interference by double-stranded RNA in *Caenorhabditis elegans*. *Nature.* 391:806–811.

Francis, G.R., and R.H. Waterston. 1991. Muscle cell attachment in *Caenorhabditis elegans. J. Cell Biol*. 114:465–479.

Fuchs, E., and D.W. Cleveland. 1998. A structural scaffolding of intermediate filaments in health and disease. *Science.* 279:514–519.

Gatewood, B.K., and E.A. Bucher. 1997. The mup-4 locus in *Caenorhabditis elegans* is essential for hypodermal integrity, organismal morphogenesis and embryonic body wall muscle position. *Genetics.* 146:165–183.

Gettner, S.N., C. Kenyon, and L.F. Reichardt. 1995. Characterization of β-pat-3 heterodimers, a family of essential integrin receptors in *C. elegans. J. Cell Biol.* 129:1127–1141.

Hall, D.H. 1995. Electron microscopy and three dimensional image reconstruction. *In Caenorhabditis elegans*: Modern Biological Analysis of an Organism. H.F. Epstein and D.C. Shakes, editors. Academic Press, San Diego, CA. 395–436.

Handford, P.A., M. Mayhew, M. Baron, P.R. Winship, I.D. Campbell, and G.G. Brownlee. 1991. Key residues involved in calcium-binding motifs in EGF-like domains. *Nature.* 351:164–167.

Henry, M.D., and K.P. Campbell. 1998. A role for dystroglycan in basement membrane assembly. *Cell.* 95:859–870.

Hong, L., T. Elbl, J. Ward, C. Franzini-Armstrong, K.K. Rybicka, B.K. Gatewood, D.L. Baillie, and E.A. Bucher. 2001. MUP-4 is a novel transmembrane protein with functions in epithelial cell adhesion in *Caenorhabditis elegans*. *J. Cell Biol.* 154:403–414.

Hresko, M.C., B.D. Williams, and R.H. Waterston. 1994. Assembly of body wall muscle and muscle cell attachment structures in *Caenorhabditis elegans*. *J. Cell Biol.* 124:491–506.

Hresko, M.C., L.A. Schriefer, P. Shrimankar, and R.H. Waterston. 1999. Myotactin, a novel hypodermal protein involved in muscle-cell adhesion in *Caenorhabditis. J. Cell Biol.* 146:659–672.

Hutter, H., B.E. Vogel, J.D. Plenefisch, C.R. Norris, R.B. Proenca, J. Spieth, C. Guo, S. Mastwal, X. Zhu, J. Scheel, and E.M. Hedgecock. 2000. Conservation and novelty in the evolution of cell adhesion and extracellular matrix genes. *Science.* 287:989–994.

Hynes, R.O. 1999. Cell adhesion: old and new questions. *Trends Cell Biol.* 9:M33–M37.

Kamiguchi, H., M.L. Hlavin, M. Yamasaki, and V. Lemmon. 1998. Adhesion molecules and inherited diseases of the human nervous system. *Annu. Rev. Neurosci.* 21:97–125.

Kowalczyk, A.P., E.A. Bornslaeger, S.M. Norvell, H.L. Palka, and K.J. Green. 1999. Desmosomes: intercellular adhesive junctions specialized for attachment of intermediate filaments. *Int. Rev. Cytol.* 185:237–302.

Kramer, J.M. 1997. Extracellular matrix. *In C. elegans* II. D.L. Riddle, T. Blumenthal, B.J. Meyer, and J.R. Priess, editors. Cold Spring Harbor Press, Cold Spring Harbor, NY. 471–500.

Mack, J.W., A.C. Steven, and P.M. Steinert. 1993. The mechanism of interaction of filaggrin with intermediate filaments. The ionic zipper hypothesis. *J. Mol. Biol.* 232:50–66.

Mello, C., and A. Fire. 1995. DNA Transformation. *In Caenorhabditis elegans*: Modern Biological Analysis of an Organism. H.F. Epstein and D.C. Shakes, editors. Academic Press, San Diego, CA. 441–482.

Mendoza, L.M., D. Nishioks, and V.D. Vacquier. 1993. A GPI-anchored sea urchin sperm membrane protein containing EGF domains is related to human uromodulin. *J. Cell Biol.* 121:1291–1297.

Miller, D.M., and D.C. Shakes. 1995. Immunofluorescence microscopy. *In Caenorhabditis elegans*: Modern Biological Analysis of an Organism. H.F. Epstein and D.C. Shakes, editors. Academic Press, San Diego, CA. 365–394.

Moerman, D.G., and A. Fire. 1997. Muscle: structure, function, and development. *In C. elegans* II. D.L. Riddle, T. Blumenthal, B.J. Meyer, and J.R. Priess, editors. Cold Spring Harbor Press, Cold Spring Harbor, NY. 417–470.

Nelson, F.K., P.S. Albert, and D.L. Riddle. 1983. Fine structure of the *Caenorhabditis elegans* secretory-excretory system. *J. Ultrastruct. Res.* 82:156–171.

Nievers, M.G., R.Q.J. Schaapveld, and A. Sonnenberg. 1999. Biology and function of hemidesmosomes. *Matrix Biol.* 18:5–17.

Peixoto, C.A., J.V. de Melo, J.M. Kramer, and W. de Souza. 1998. Ultrastructural analysis of the *Caenorhabditis elegans* rol-6(su1006) mutant, which produces abnormal cuticle collagen. *J. Parasitol.* 84:45–49.

Perl, A.K., P. Wilgenbus, U. Dahl, H. Semb, and G. Christofori. 1998. A causal role for E-cadherin in the transition from adenoma to carcinoma. *Nature.* 392:190–193.

Perkins, L.A., E.M. Hedgecock, J.N. Thompson, and J.G. Culotti. 1986. Mutant sensory cilia in the nematode *Caenorhabditis elegans*. *Dev. Biol.* 117:456–487.

Plenefisch, J.D., X. Zhu, and E.M. Hedgecock. 2000. Fragile skeletal muscle attachments in dystrophic mutants of *Caenorhabditis elegans*: isolation and characterization of the *mua* genes. *Development.* 127:1197–1207.

Prout, M., Z. Damania, J. Soong, D. Fristrom, and J.W. Fristrom. 1997. Autosomal mutations affecting adhesion between wing surfaces in *Drosophila* melanogaster. *Genetics.* 146:275–285.

Riddle, D.L., T. Blumenthal, B.J. Meyer, and J.R. Preiss, editors. 1997. *C. elegans* II. Cold Spring Harbor Laboratory Press, Cold Spring Harbor, NY. 1222 pp.

Rubin, G.M., M.D. Yandell, J.R. Wortman, G.L. Gabor Miklos, C.R. Nelson, I.K. Hariharan, M.E. Fortini, P.W. Li, R. Apweiler, W. Fleischmann, et al. 2000. Comparative genomics of the eukaryotes. *Science.* 287:2204–2215.

Russell, D.W., M.S. Brown, and J.L. Goldstein. 1989. Different combinations of cysteine-rich repeats mediate binding of low density lipoprotein receptor to two different proteins. *J. Biol. Chem.* 264:1682–1688.

Tepass, U., and V. Hartenstein. 1993. The development of cellular junctions in the *Drosophila* embryo. *Dev. Biol.* 161:563–596.

Waterston, R.H. 1988. Muscle. *In* The Nematode *Caenorhabditis elegans*. W. Wood, editor. Cold Spring Harbor Laboratory Press, Cold Spring Harbor, NY. 281–333.

Williams, B.D., and R.H. Waterston. 1994. Genes critical for muscle development and function in *Caenorhabditis elegans* identified through lethal mutations. *J. Cell Biol.* 124:475–490.

White, J.G. 1988. The anatomy. *In* The Nematode *Caenorhabditis elegans*. W. Wood, editor. Cold Spring Harbor Laboratory Press, Cold Spring Harbor, NY. 81–122.